Electronic supplementary information

Pillar effect on cyclability enhancement for aqueous lithium ion batteries: a new anode material of β-vanadium bronze $M_{0.33}V_2O_5$ (M=Ag, Na) nanowires

Yang Xu,[a] Xiaosan Han,[a] Lei Zheng,[a] Wensheng Yan[b] and Yi Xie*[a]

[a] Hefei National Laboratory for Physical Sciences at the Microscale,
University of Science & Technology of China, Hefei, Anhui 230026, P.R. China.
Fax : (+86)-551-360-6266, Tel : (+86)-551-360-3987, E-mail : yxie@ustc.edu.cn
[b] National Synchrotron Radiation Laboratory,
University of Science & Technology of China, Hefei, Anhui 230029, P.R. China.

S1. XRD pattern and SEM image of $AgVO_3$ precursor

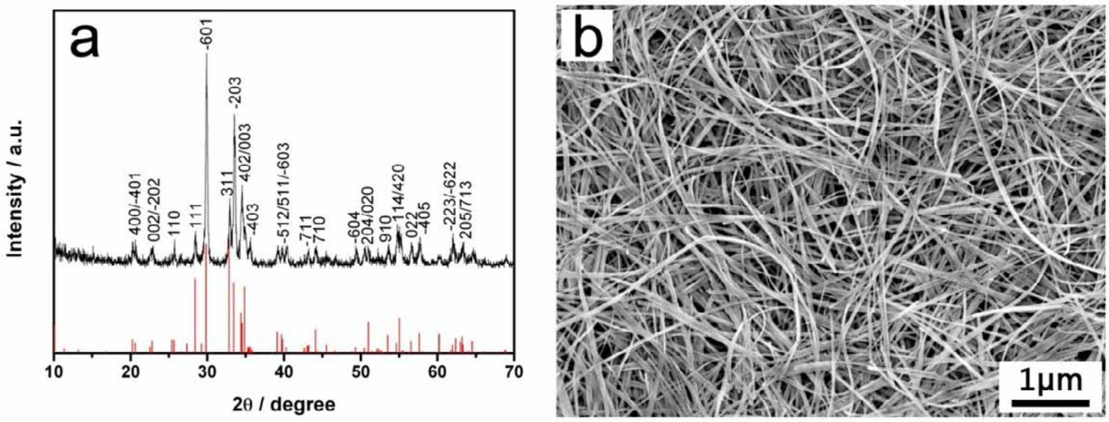

Fig. S1 (a) XRD pattern and (b) SEM image of $AgVO_3$ precursor.

All diffraction peaks in XRD pattern (Fig. S1a) can be indexed as monoclinic $AgVO_3$ (a=18.106 Å, b=3.579 Å, c=8.043 Å, and β=104.44°) which is consistent with the values given by JCPDS card No.86-1154. No peaks from other phases can be detected. The SEM image (Fig. S1b) shows that the precursor consists of a large quantity of uniform 1D nanowires with the diameters of ~100 nm and typical lengths up to several tens of micrometers.

S2. XRD pattern and SEM image of $Ag_2V_4O_{11}$ nanobelts

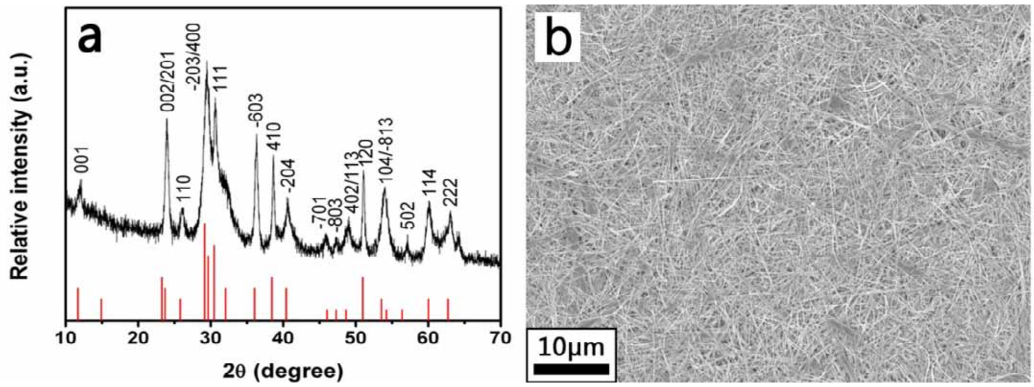

Fig. S2 (a) XRD pattern and (b) SEM image of $Ag_2V_4O_{11}$ nanobelts.

All diffraction peaks in XRD pattern (Fig. S2a) can be indexed as monoclinic $Ag_2V_4O_{11}$ ($a=15.33$ Å, $b=3.587$ Å, $c=9.526$ Å, and $\beta=127.9°$), which is consistent with the values given by JCPDS card No.49-0166. The SEM image (Fig. S2b) shows a typical panoramic view that a large number of nanobelts with the average diameter of 70~80 nm and length of about several tens of micrometers are distributed homogeneously over a wide area.

S3. EDX spectrum of the as-obtained $Ag_{0.33}V_2O_5$ nanowires

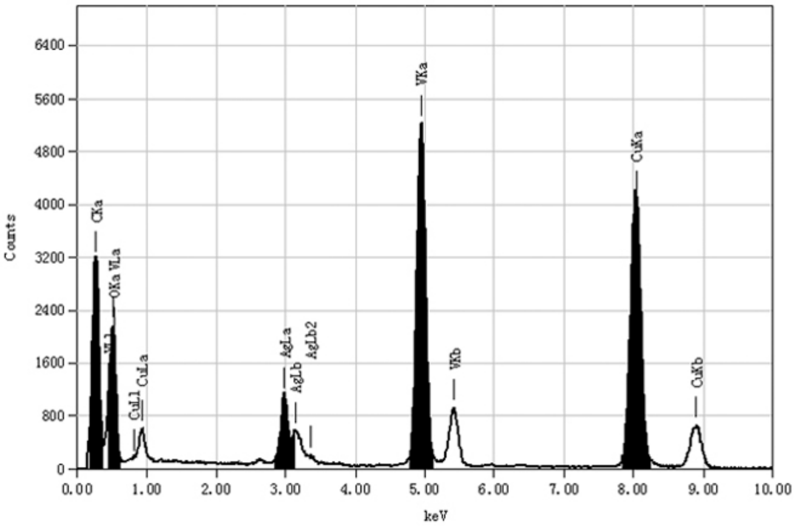

Fig. S3 EDX spectrum of the as-obtained $Ag_{0.33}V_2O_5$ nanowires.

S4. Discharge capacity retention and XRD patterns of $Ag_2V_4O_{11}$ nanobelts before and after charge-discharge test

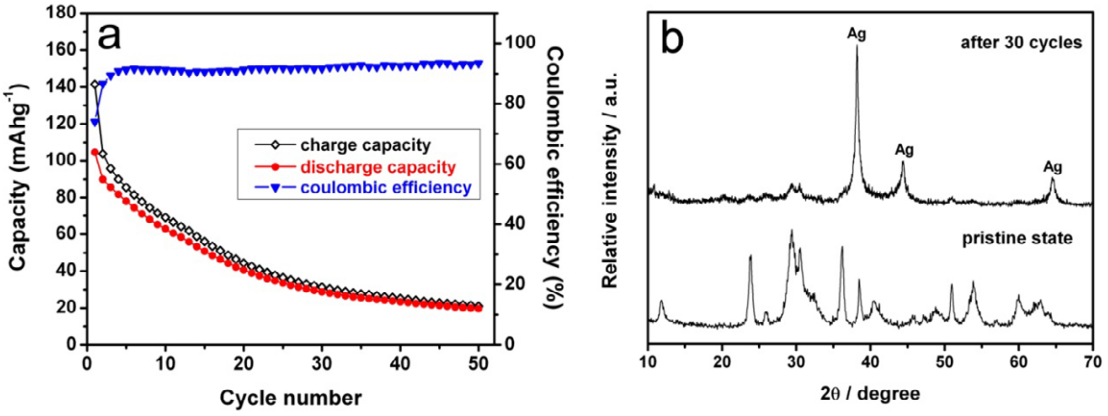

Fig. S4 (a) Charge/discharge capacity and coulombic efficiency versus cycle number curves of the $LiMn_2O_4/Ag_2V_4O_{11}$ cell. The cell was charged and discharged at the current density of 60 mA g^{-1} in aqueous electrolyte. (b) XRD patterns of $Ag_2V_4O_{11}$ nanobelts in pristine state and after 30 cycles.

As shown in Fig. S4a, the first discharge capacity of $Ag_2V_4O_{11}$ nanobelts is 104.6 mA h g^{-1} which is close the value of $Ag_{0.33}V_2O_5$ nanowires in the manuscript (103.2 mA h g^{-1}), but the retention decreases rapidly from 85.9% after 2 cycles to 27.5% after 30 cycles, and eventually 18.7 % after 50 cycles, showing much worse cycle performance than $Ag_{0.33}V_2O_5$ nanowires (53.2% after 100 cycles). The XRD pattern of $Ag_2V_4O_{11}$ nanobelts after 30 cycles (Fig. S4b) clearly displays that severe amorphization occurred during repetitive lithiation due to the collapse of V-O slabs arising from the significant ionic radii mismatch between silver and lithium ions (r_{Ag^+} = 1.15 Å and r_{Li^+} = 0.76 Å).

S5. Characterization of the as-obtained $Na_{0.33}V_2O_5$ nanowires

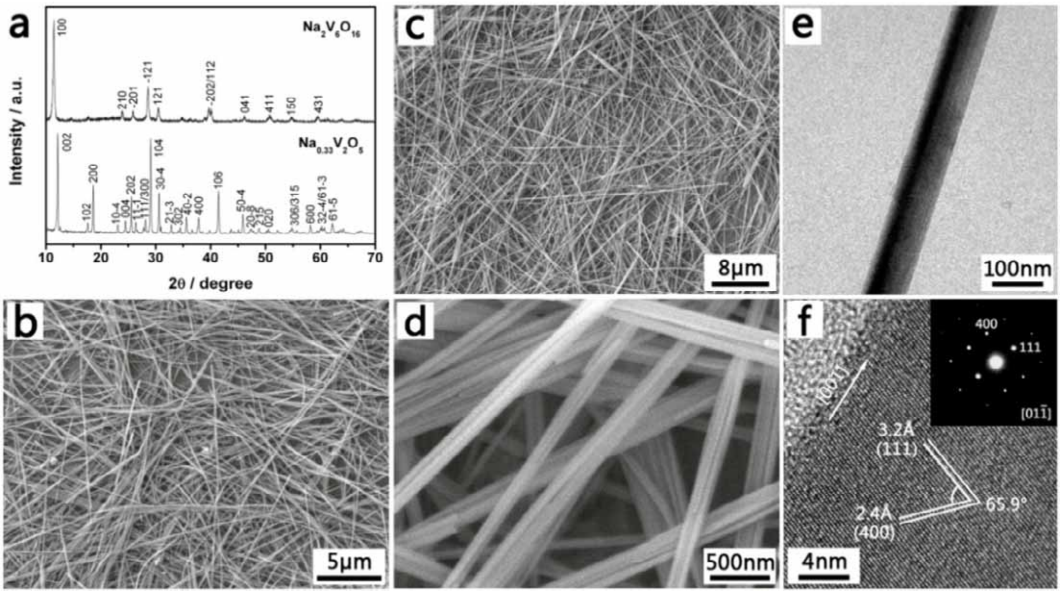

Fig. S5 (a) XRD patterns of $Na_2V_6O_{16}$ precursor and the corresponding product $Na_{0.33}V_2O_5$. (b) SEM image of $Na_2V_6O_{16}$ nanowires. (c, d) SEM images, (e) TEM image, and (f) HRTEM image and SAED pattern of the as-obtained $Na_{0.33}V_2O_5$ nanowires.

As shown in Fig. S5a, all diffraction peaks of precursor and product can be indexed as monoclinic $Na_2V_6O_{16}$ (a=8.37 Å, b=8.56 Å, c=5.07 Å, and β=96.75°) and monoclinic $Na_{0.33}V_2O_5$ (a=10.088 Å, b=3.617 Å, c=15.449 Å, and β=109.57°), which are consistent with the values given by JCPDS card No.22-1412 and 86-0120, respectively. Both precursor and product consist of a large quantity of uniform 1D nanowires with the diameters of 100~120 nm and typical lengths up to several tens of micrometers (Fig. S5b-d). The morphological yield is nearly 100% and good morphological heritage can be clearly observed. The TEM image (Fig. S5e) of representative single nanowire further demonstrates that the as-obtained product has a uniform wire-like morphology. SAED analysis taken from the single nanowire reveals its single crystalline nature. The HRTEM image (Fig. S5f) shows the clearly resolved lattice fringes, corresponding to the (111) and (400) planes of $Na_{0.33}V_2O_5$, respectively. The angles between these planes are 65.9° which is consistent with the SAED pattern. The $Na_{0.33}V_2O_5$ nanowire shows a preferred [001] orientation.

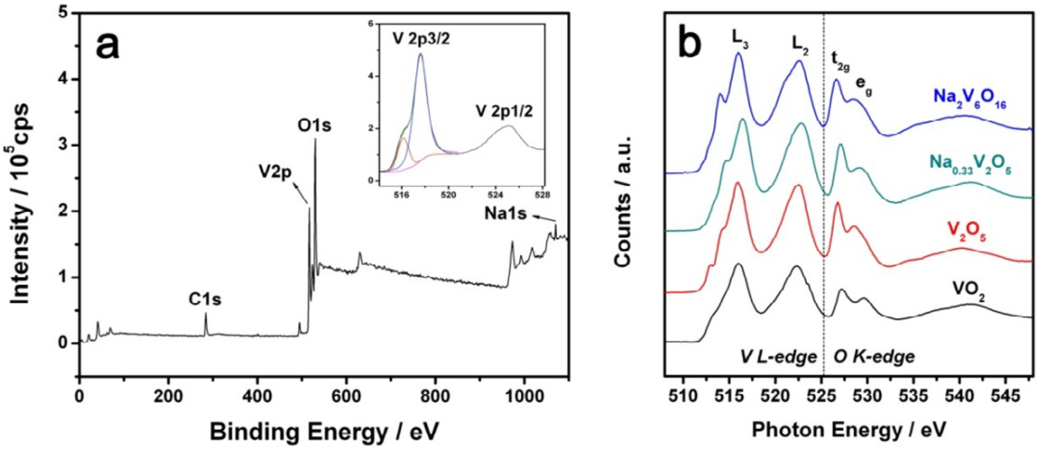

Fig. S6 (a) XPS survey spectrum (inset: V high resolution spectrum) of the as-obtained $Na_{0.33}V_2O_5$ nanowires. (b) NEXAFS data for $Na_2V_6O_{16}$ precursor, the $Na_{0.33}V_2O_5$ sample, commercial V_2O_5 and VO_2.

XPS spectrum (Fig. S6a) shows the dominant ingredients of vanadium, oxygen and sodium for the as-obtained sample. The existence of mixed vanadium valence is clearly confirmed by the overlapping peaks of V^{4+} and V^{5+} in V 2p core level spectra (inset of Fig. S6a). NEXAFS data of the smaple (Fig. S6b) exhibits the same characters as that of $Ag_{0.33}V_2O_5$ nanowires in Fig. 3 of the manuscript, providing strong evidence for charge disproportionation in the structure of $Na_{0.33}V_2O_5$ which is attributed to the presence of mixed vanadium valence.